



OPEN

Enhancing impact resistance and biodegradability of PHBV by melt blending with ENR

Napat Tomano¹, Orathai Boondamnoen²✉, Chuanchom Aumnate^{3,4}✉ & Pranut Potiyaraj^{2,3,4}

This research aims to enhance the mechanical characteristics of poly(3-hydroxybutyrate-co-3-hydroxyvalerate) (PHBV) by using epoxidized natural rubber (ENR-25 and ENR-50) as a toughening agent and polybutadiene (PB) grafted with maleic anhydride (MA) (3 MA groups/chain) as a compatibilizer. The PHBV/ENR blends were mixed in 100/0, 90/10, 80/20, and 70/30 with PB-g-MA at 0, 5, and 10% (wt./wt.), using an internal mixer set to 175 °C with a rotor speed of 50 rpm. The findings indicated that at 70/30 PHBV/ENR composition, the impact strength of the blends with 25 and 50 epoxide contents were the greatest at $6.92 \pm 0.35 \text{ J m}^{-1}$ and $7.33 \pm 1.19 \text{ J m}^{-1}$, respectively, which are about two times greater than that of neat PHBV. Furthermore, the biodegradability of the PHBV/ENR blends was more substantial than that of neat PHBV, showing a mass reduction of approximately 40% and 45% for PHBV/ENR-25 and PHBV/ENR-50, respectively. In comparison, while the mass loss of PHBV was approximately 37% after three months of soil burial. The results indicate that ENR improves the toughness of the blends while simultaneously increasing PHBV degradation, which could pave the way for broadening PHBV for sustainability purposes.

In recent years, petroleum-based products have been one of the most worrying environmental issues since the causes cannot be regenerated, and they are resistant to biological, physical, and chemical degradation¹. That has a significant role in the causes of environmental problems like global warming and the loss of a diverse range of organisms in the world's ecosystem and habitat². Thus, bio-based materials have been developed to replace petroleum-based materials and are potentially utilized for commercial products³. Biodegradable plastics, the bio-based materials that could be sourced from nature and degraded spontaneously by microbial activity, such as poly(3-hydroxybutyrate), (PHB) and poly(3-hydroxybutyrate-co-3-hydroxyvalerate), (PHBV), which are also known as biodegradable aliphatic polyester in a group of poly(3-hydroxyalkanoates) (PHAs)^{4,5}. PHAs can be produced through the fermentation process of bacteria such as *Alcaligenis eutrophus*, *Bacillus*, and *Pseudomonas* in an oxygen and carbon dioxide regulated environment⁶⁻⁹. Interestingly, it rapidly decomposes into water and carbon dioxide¹⁰.

PHBV is a promising bioplastic used in various biomedical applications, such as drug-delivery carriers, scaffolds, bone repair, orthopedic devices, and the packaging industry. Also, PHBV is generally tougher than PHB because of its chemical functionalization. However, one of the critical drawbacks is its thermal instability, which could bring about a narrow processing window. The degradation of PHBV could be rapidly accelerated during conventional processing methods such as melt extrusion and injection molding, resulting in restricted PHBV usage¹¹. Moreover, the high crystallinity of up to 70% and slow nucleation rate make PHBV brittle, leading to poor mechanical characteristics¹². Thus, many studies have been undertaken to explore strategies to enhance physical and functional properties, which could strengthen the possibility of PHBV as sustainable packaging material. Blending PHBV with other polymers is a proposed solution to reduce crystallinity and improve toughness^{13,14}. Besides, it is not only for enhancing the mechanical performance, but biodegradability is also preserved. Many approaches for toughening PHBV have been suggested, such as thermal treatment modification via annealing to decrease crystallinity¹⁵ and blending with other flexible polymers, such as PBS¹⁶. However, the compatibility between PHBV and the blending polymer is a critical concern; for example, the compatibility between PHBV and PBS was poor due to relatively large particle size and weak interfacial adhesion in their blends. The same phenomenon was observed for PHBV/Polybutylene adipate terephthalate (PBAT) blends¹⁷. Moreover, it was

¹Nanoscience and Technology Program, Graduate School, Chulalongkorn University, Bangkok 10330, Thailand. ²Department of Materials Science, Faculty of Science, Chulalongkorn University, Bangkok 10330, Thailand. ³Metallurgy and Materials Science Research Institute, Chulalongkorn University, Bangkok 10330, Thailand. ⁴Center of Excellence in Responsive Wearable Materials, Chulalongkorn University, Bangkok 10330, Thailand. ✉email: Orathai.b@chula.ac.th; Chuanchom.a@chula.ac.th

reported that the addition of PBAT led to a decrease in crystallinity consistently with increasing PBAT composition in the blends.

Among various polymers, natural rubber (NR) is a promising sustainable toughening agent from renewable natural resources with high molecular weight, low glass transition temperature, flexibility, and ductility¹⁸. Epoxidized natural rubber (ENR) is a chemically modified natural rubber from epoxidation process. Herein, the double bonds of isoprene units are replaced with epoxide groups¹⁹. The degree of epoxidation may be effectively controlled by time processing, with 25 and 50 mol% almost being utilized. Commercially available ENR with 25 and 50 mol% epoxy contents are named ENR-25 and ENR-50, respectively. The epoxide group content is projected to significantly impact the reactivity to blending with polymers than natural rubber²⁰. ENR is more compatible with polymers containing polar functional groups, such as PHBV. The effect of ENR and NR as toughening agents for PHB was studied. It was reported that the addition of 40% ENR increased the toughness of the PHB/ENR blend, while the PHB/NR blend did not show an improved toughness. This may be attributed to the produced unbonded rubber phase in PHB/NR blends. Also, it was reported that the blending of PHBV/ENR exhibits good compatibility with further improved toughness compared to the PHBV/NR blend^{21,22}.

In addition, adding compatibilizers is one of the effective attempts to improve the compatibility of blending PHBV with other polymers. It could prevent coalescence and enhance interfacial adhesion, thus reducing the phase separation between blending compositions²³. Maleated polybutadiene is a compatibilizer applied for PHB/ENR blends. With its high grafting and low molecular weight, the interfacial adhesion between the PHB and ENR could be achieved, thus improving the toughness characteristic of the blends^{22,24,25}. However, the effect of adding compatibilizers on improving the properties of PHBV/ENR blends has rarely been reported.

This study aims to improve the toughness of PHBV by melt-blending with different epoxidized rubbers, ENR-25, and ENR-50, using an internal mixer. Herein, the effect of epoxide contents and compatibilizer (PB-g-MA) on improving the mechanical properties of the PHBV/ENR blends was investigated in terms of notched impact strength, tensile properties, and flexural properties. The thermal behaviors of the blends were examined by thermogravimetric analysis (TGA) and differential scanning calorimetry (DSC), respectively. The crystal structure was monitored by x-ray Diffraction (XRD) analysis. Also, the blend morphology was studied by scanning electron microscopy (SEM). Moreover, the biodegradability of the PHBV/ENR blends was also investigated by burying them in the soil for three months.

Results and discussion

Figure 1 presents the probable reactions during the melt-blending process with and without a compatibilizer. The reaction begins with a random thermal scission of long-chain PHBV molecules to shorter chains containing carboxyl ends^{15,26}, as shown in Eq. (1). In the presence of ENR, the epoxide ring in the vicinity of the newly generated carboxyl groups was open as Eq. (2). It is important to note that the hydroxyl group is thus produced and reactive towards the carboxyl and epoxide groups. When the reaction was completed, water was found as a byproduct. The potential reaction pathway of the blends using PB-g-MA as a compatibilizer begins with the ring-opening of maleic anhydride by heat reacting with water to create hydroxyl groups, as shown in (3)²⁷. Finally, the obtained product from the reaction as Eq. (3) reacts at the oxirane ring of ENR and the carboxyl of PHBV, as shown in Eq. (4)²⁸.

Thermal stability. Figure 2 presents the TGA thermogram of the neat PHBV (100/0), and PHBV/ENR blends with and without compatibilizer (PB-g-MA). It was observed that PHBV/ENR blends were degraded in two stages, revealing the differences in the thermal stability of PHBV and ENR. The first stage demonstrated PHBV decomposition between 254.3 and 304.0 °C²⁶, whereas the second stage, between 272.8 and 460.0 °C and between 280.8 and 460.0 °C²⁹, revealed the decomposition for ENR-25 and ENR-50, respectively. During the melt-blending process, the thermal could accelerate random chain scission of PHBV, creating olefinic compound, carboxylic acid, crotonic acid, and oligomer³⁰. PHBV could also depolymerize to decrease molecular weight by acid from random chain scission reaction. The higher the ENR content, the more significant deterioration, which may be attributed to the more heat dissipation of ENR³¹. As a result, the thermal stability of the blends tended to be reduced with the ENR loading. On the other hand, the degradation temperature of the ENR counterpart was enhanced in proportion to higher ENR concentration, attributing to the interaction with PHBV surrounding the ENR phase retarding ENR degradation. Nevertheless, less thermal stability was observed for the blends with 5% PB-g-MA. This may be ascribed to the higher compatibility level between PHBV and ENR, which resulted in a smaller phase distribution of ENR, thus inducing more heat dissipation to PHBV^{32,33}. For all blend compositions, the blends with ENR-50 exhibited slightly higher thermal stability than those with ENR-25 because of higher epoxidation content³⁴.

Thermal properties. Figure 3 displays the second heat DSC thermogram of PHBV and its blends. The glass transition temperature (T_g) for all PHBV/ENR blends was not observed due to the high crystallinity of PHBV. A single melting temperature (T_m) peak was presented at 171.1 °C for the neat PHBV (100/0). For all blends, the broader T_m peaks ranged from 164.0 to 172.4 °C. Incorporating ENR seems to have significant effects on the crystallization behavior of the blends. The increase in the ENR loading, the lower the T_m . Moreover, increasing the ENR loadings resulted in a broader melting peak and lower degree of crystallinity (X_c), particularly for blends with 30 w% of ENR content (for both ENR-25 (a) and ENR-50 (b)). The transition temperatures and the parameters obtained from the DSC measurement of PHBV/ENR blends are demonstrated in Table 1. The melting and crystallization behaviors of polymer blends were significant in deciding mechanical properties³⁵. The decrease in crystallization temperatures (T_c) and the degree of crystallization (X_c) may be associated with the development of imperfect crystallites. The possibility of the ENR phase migrating into the inter- and intra-spherulitic regions

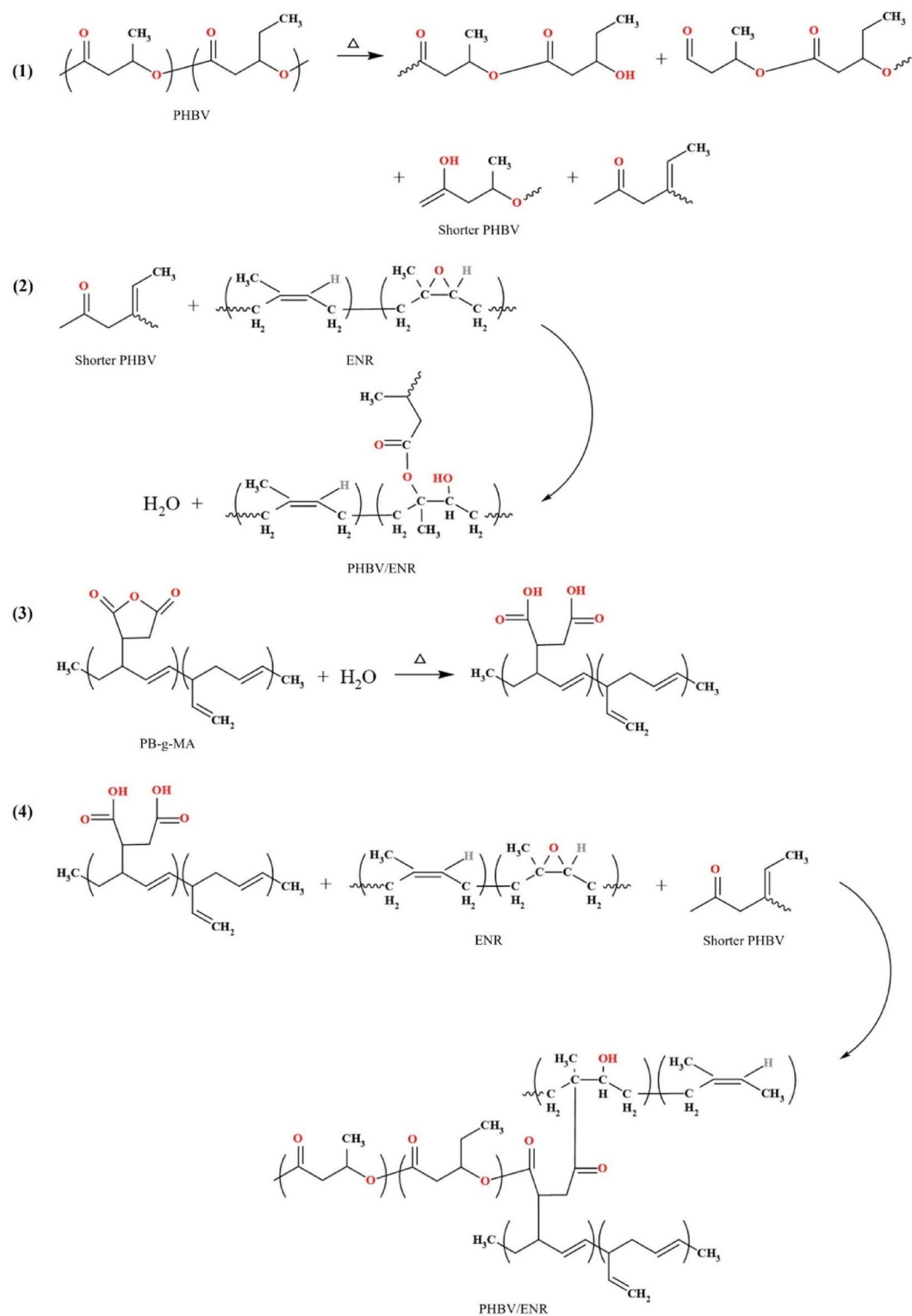


Figure 1. Schematic illustration of the proposed reactions between PHBV, ENR, and PB-g-MA.

of crystalline PHBV restricted the crystal development from its preferred crystalline morphology^{36,37}. Moreover, the compatibility of PHBV/ENR blends with a compatibilizer (5wt% PB-g-MA) resulted in a lower interfacial contact area between the PHBV and ENR phases. As a result, the polymer networks could be generated, thus inhibiting PHBV crystallization^{38–40}.

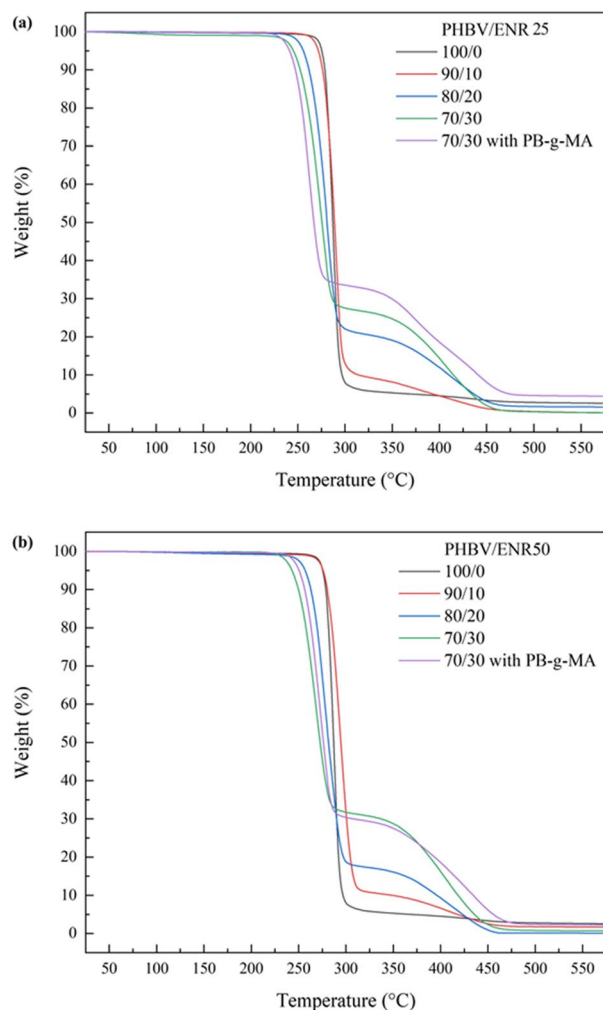


Figure 2. The TGA thermogram of neat PHBV (100/0) and PHBV/ENR blends with and without compatibilizer (PB-g-MA), (a) PHBV/ENR-25 blends, and (b) PHBV/ENR-50 blends.

Crystal structure. The XRD diffractograms of PHBV and all blends are shown in Fig. 4. The orthorhombic crystal structure was shown by reflection peaks at 13.25° , 16.63° , 25.17° , and 26.52° , which correspond to the (020), (110), (031), and (040) planes⁴¹. Nonetheless, the degree of crystallinity of the blends was considerably reduced, confirming the DSC results. No new peak was detected in the XRD patterns for all blends, showing no new crystalline phase occurred⁴². Compared with the neat PHBV (PHBV unprocessed), the planes of (020), (110), (031), and (040) were shifted to higher angles and broader for all blends. This could be described as the crystal growth of PHBV in the blends being restricted by the dispersed ENR phase, suggesting that the melt-blending with ENR significantly reduced the crystallinity of the PHBV⁴³. Similar results were found for either blending with ENR-25 or ENR-50.

Mechanical properties. The mechanical properties of polymer blends are directly governed by their compatibility between blending compositions⁴⁴. This section discussed the effect of PB-g-MA loadings, 5wt%, and 10wt%, on the blends' mechanical properties. Tables 2 and 3 present the mechanical properties of the PHBV and blends with ENR-25 and ENR50, respectively.

Tensile properties. The ENR diminished tensile strength and Young's modulus of the blends because of the softening effect of the ENRs, and voids formation in their structures⁴⁵ due to the compatibility between PHBV and ENR. During the melt blending process, PHBV chains were broken into shorter chains before reacting with the compatibilizer and ENR (see Fig. 1), reducing the crystallinity and directly affecting the tensile characteristics. As shown in Fig. 5, for the PHBV/ENR-25 blends, the tensile strength significantly decreases with increasing the ENR-25 content due to the rubber's low modulus and strength characteristics^{46,47}. The addition of a compatibilizer, PB-g-MA, significantly improved the tensile strength of the blends with 10wt% ENR-25 content. However, for higher ENR-25 contents, 20 and 30wt%, the presence of PB-g-MA has no significant effect on improving the tensile strength of the blends. For PHBV/ENR-50 blends, the presence of compatibilizer signifi-

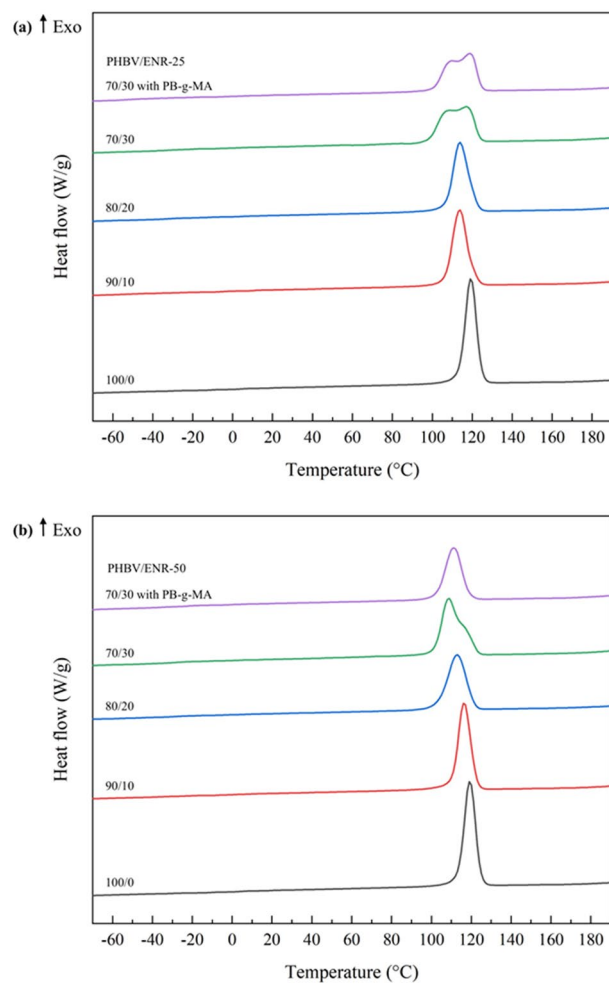


Figure 3. The second heat DSC thermogram of PHBV (100/0) and PHBV/ENR blends with and without compatibilizer (PB-g-MA), (a) PHBV/ENR-25 blends and (b) PHBV/ENR-50 blends.

Samples	T_c (°C)	T_m (°C)	ΔH_c (J g ⁻¹)	ΔH_m (J g ⁻¹)	X_c (%)
PHBV (100/0)	119.3	171.1	92.0	91.6	84.0
PHBV/ENR-25					
90/10	113.7	171.4	85.1	95.6	87.7
80/20	113.8	167.6	80.7	86.6	79.4
70/30	117.0	167.6	77.3	86.7	79.6
70/30 with PB-g-MA	118.8	168.1	74.3	77.8	71.4
PHBV/ENR-50					
90/10	116.4	172.4	84.5	91.6	84.1
80/20	112.8	167.6	75.9	82.3	69.7
70/30	108.7	164.0	83.9	91.6	84.0
70/30 with PB-g-MA	111.2	169.8	65.2	71.7	65.7

Table 1. DSC parameters of PHBV and PHBV/ENR blends.

cantly improved the tensile strength of all blends. A significant tensile strength improvement was observed for the blends with 10wt% PB-g-MA addition. It is worth noting that the higher the PB-g-MA content, the higher the tensile strength achieved due to the compatibility between PHBV and ENR induced by the content of epoxy-oxidation. A similar phenomenon was also observed for Young's modulus.

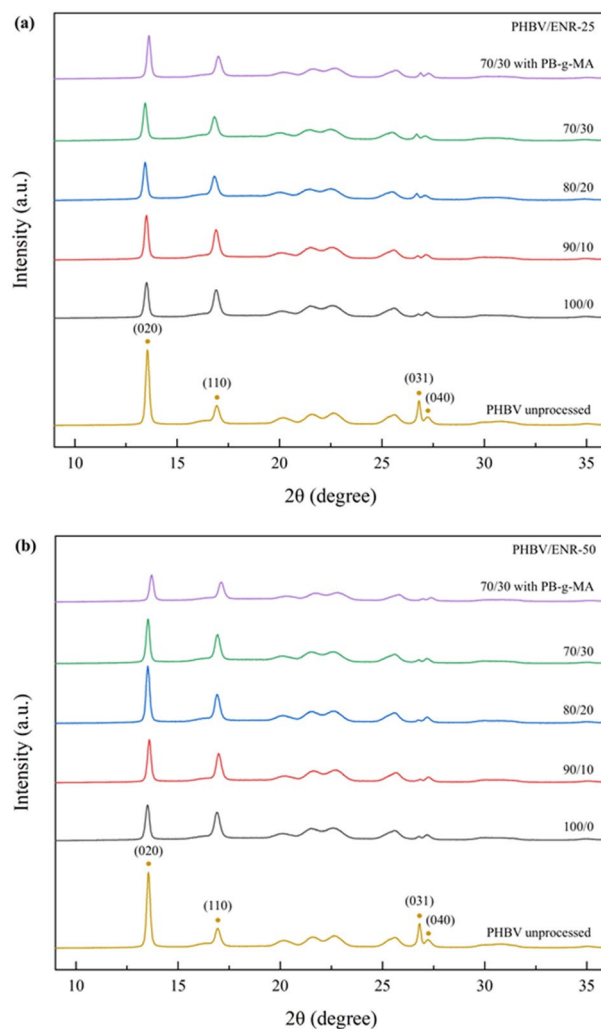


Figure 4. XRD diffractograms of the neat PHBV (PHBV unprocessed) and PHBV/ENR blends (a) PHBV/ENR-25 blends and (b) PHBV/ENR-50 blends.

Samples	Compatibilizer (%)	Impact strength (J/m)	Tensile properties			Flexural modulus (MPa)	Strain (%)
			Tensile strength (MPa)	Elongation at break (%)	Young's modulus (MPa)		
100 PHBV	–	3.30 ± 0.66	28.34 ± 3.37	6.65 ± 0.73	868.29 ± 149.77	3,020.89 ± 178.00	4.14 ± 0.81
PHBV/ENR-25							
90/10	–	4.72 ± 0.10	21.98 ± 2.44	5.51 ± 0.62	851.79 ± 36.00	2,287.90 ± 59.36	6.72 ± 0.52
80/20	–	5.51 ± 0.56	13.85 ± 1.93	2.70 ± 0.18	689.78 ± 39.39	1,775.94 ± 65.37	7.10 ± 0.66
70/30	–	6.76 ± 0.43	5.60 ± 1.09	5.47 ± 0.66	343.59 ± 76.89	671.25 ± 47.03	8.09 ± 1.19
PHBV/ENR-25/5%PB-g-MA							
90/10	5	3.30 ± 0.86	25.83 ± 1.43	5.35 ± 0.49	802.71 ± 53.78	2,655.55 ± 96.24	5.24 ± 0.47
80/20	5	4.72 ± 0.97	15.01 ± 1.03	3.56 ± 0.12	655.82 ± 24.41	1,760.64 ± 61.46	6.09 ± 0.66
70/30	5	6.92 ± 0.35	4.70 ± 0.60	3.36 ± 0.22	315.90 ± 4.52	1,240.33 ± 192.55	7.63 ± 0.89
PHBV/ENR-25/10% PB-g-MA							
90/10	10	1.57 ± 0.10	28.00 ± 2.92	6.02 ± 1.21	819.74 ± 75.96	2,512.57 ± 91.43	4.81 ± 0.26
80/20	10	2.99 ± 0.66	14.06 ± 1.98	2.88 ± 0.41	637.43 ± 52.53	1,837.75 ± 90.52	5.32 ± 0.46
70/30	10	4.56 ± 0.66	5.67 ± 0.60	2.63 ± 0.61	361.97 ± 53.15	825.72 ± 52.49	5.78 ± 0.72

Table 2. Mechanical properties of the PHBV and PHBV/ENR-25 blends.

Samples	Compatibilizer (%)	Impact strength (J/m)	Tensile properties			Flexural modulus (MPa)	Strain (%)
			Tensile strength (MPa)	Elongation at break (%)	Young's modulus (MPa)		
100 PHBV	–	3.30 ± 0.66	28.34 ± 3.37	6.65 ± 0.73	868.29 ± 149.77	3,020.89 ± 178.00	4.14 ± 0.81
PHBV/ENR-50							
90/10	–	5.04 ± 0.43	22.64 ± 2.41	6.57 ± 0.61	751.70 ± 43.87	2,670.14 ± 81.03	6.09 ± 0.63
80/20	–	5.19 ± 0.43	12.58 ± 1.96	2.95 ± 0.66	652.04 ± 76.78	1,769.67 ± 58.47	6.46 ± 0.58
70/30	–	5.66 ± 1.17	8.24 ± 1.65	2.31 ± 0.68	534.33 ± 6.02	1,285.12 ± 92.16	6.81 ± 0.92
PHBV/ENR-50/5%PB-g-MA							
90/10	5	3.46 ± 0.71	22.46 ± 2.59	6.14 ± 1.20	712.49 ± 73.36	2,733.01 ± 19.17	5.08 ± 0.22
80/20	5	4.13 ± 0.98	17.40 ± 1.40	4.39 ± 0.62	655.65 ± 73.88	1,813.33 ± 49.84	6.36 ± 1.01
70/30	5	7.33 ± 1.19	5.55 ± 1.18	3.98 ± 1.35	328.41 ± 32.40	1,236.34 ± 143.46	8.29 ± 0.61
PHBV/ENR-50/10% PB-g-MA							
90/10	10	2.20 ± 0.35	27.28 ± 2.16	5.36 ± 0.63	844.05 ± 37.76	2,390.16 ± 95.70	5.45 ± 0.72
80/20	10	3.46 ± 0.43	19.29 ± 1.57	4.50 ± 0.35	644.01 ± 66.95	1,763.56 ± 52.36	6.99 ± 0.37
70/30	10	4.72 ± 1.11	10.59 ± 0.93	3.43 ± 0.58	407.06 ± 75.13	1,186.28 ± 90.60	7.32 ± 0.44

Table 3. Mechanical properties of the PHBV and PHBV/ENR-50 blends.

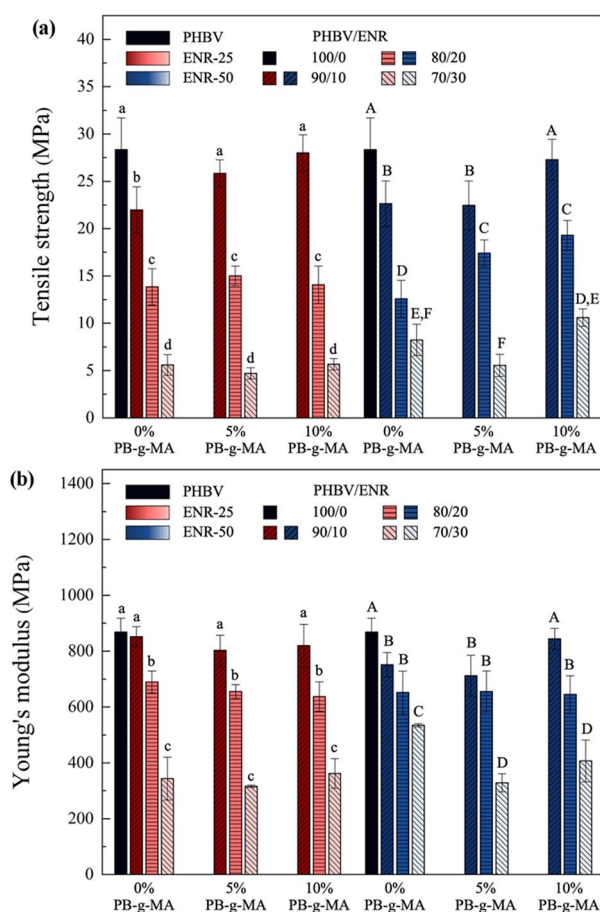


Figure 5. The tensile properties of PHBV/ENR blends (a) Tensile strength and (b) Young's modulus. Data are presented as mean ± SD. Groups designated with different letters are significantly different using One-Way ANOVA with Duncan's multiple range post hoc (at $p < 0.05$, $n = 3$).

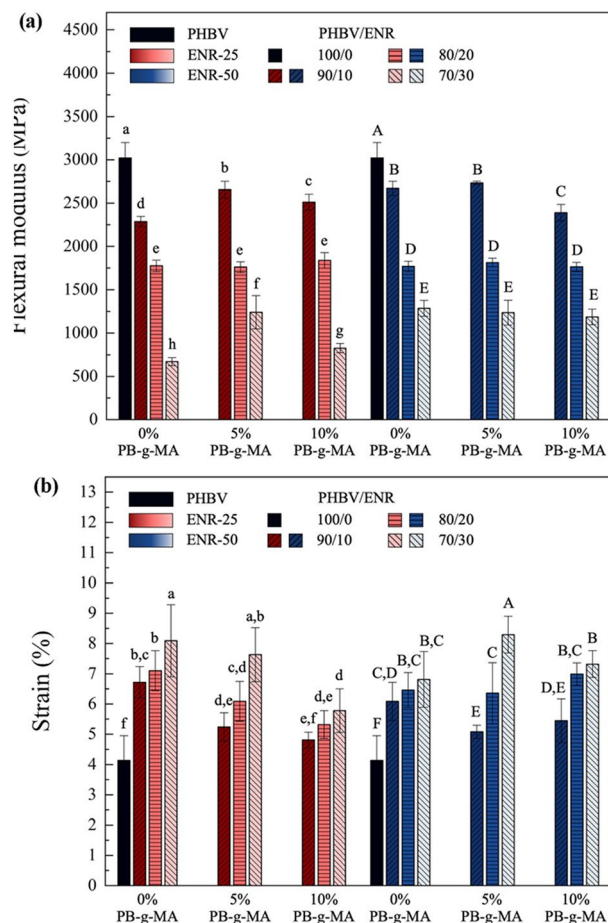


Figure 6. The flexural properties of PHBV/ENR blends (a) Flexural modulus and (b) Strain at break. Data are presented as mean \pm SD. Groups designated with different letters are significantly different using One-Way ANOVA with Duncan's multiple range post hoc (at $p < 0.05$, $n = 3$).

Flexural properties. Good compatibility of PHBV and ENRs, resulting from physical or chemical interactions, is crucial to achieving the desired mechanical properties. The flexural modulus of the blends significantly decreased with increasing ENR loading. However, the strain at break increased, as shown in Fig. 6. This is due to the low modulus and flexible nature of ENR^{48,49} in the blends. As demonstrated in Fig. 1, the part of the PHBV chain could be cross-linked with the ENR chain using PB-g-MA as a compatibilizer. The separation between PHBV and ENR phases may cause an initial crack propagation that governs the mechanical performance of the blends. The compatibilizer, PB-g-MA, could induce the chemical interaction between PHBV and ENR, thus increasing the strain at break. For PHBV/ENR-50, the addition of PB-g-MA showed a significant improvement in the strain at break, particularly in the blends with ENR contents larger than 10wt%. The most promising mechanical properties were obtained from PHBV/ENR-50 (70/30) with 5wt% PB-g-MA.

Impact properties. Notched impact strength is utilized to evaluate materials' toughness (impact resistance)⁴⁵. Figure 7 presents the impact strength of the neat PHBV and PHBV/ENR blends with and without PB-g-MA addition. The impact strength of the neat PHBV is $3.33 \pm 0.66 \text{ J m}^{-1}$, exhibiting the brittleness characteristic due to its high crystallinity. However, the impact strength was significantly increased with ENR incorporation ranging from 10 to 30wt% because of the elastomeric behavior of ENR²⁰. The impact strength increased with the ENR loading. At a small ENR concentration (10 wt%), the ENR phase was too far from each other to retain enough stress concentration to improve toughness⁵⁰. However, when the ENR content reached 30wt%, the ENR fragmented into small phases and was distributed well in PHBV, yielding toughness enhancement⁵¹. The smaller size of ENR enhances the impact strength due to good interfacial adhesion (although the average particle diameter was larger than $1 \mu\text{m}$). These results confirmed that the ENR could be used as an impact modifier or toughening agent for PHBV.

The addition of compatibilizer (PB-g-MA) significantly improved the impact strength, particularly at 5wt% loading. The blends with 30 wt% ENR-50 and 5 wt% PB-g-MA contents showed the highest toughness modification. It should be noted that the more considerable amount of PB-g-MA (10 wt%) seems to give a worse result, which may be due to the exceeded amount of PB-g-MA causing the interaction between maleic anhydride of PB-g-MA, carboxyl of PHBV, and epoxide of ENR instead of creating the interfacial adhesion between PHBV and

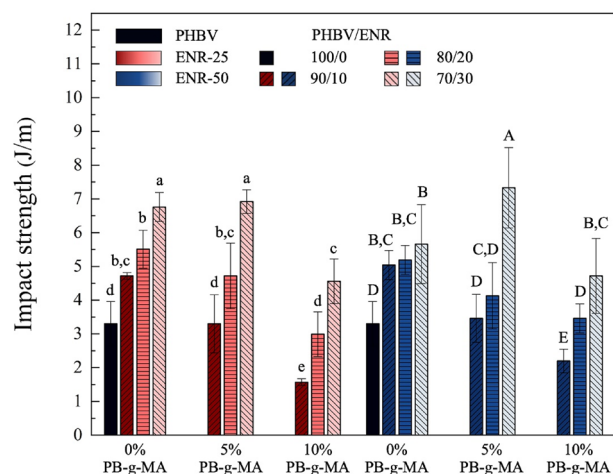


Figure 7. The impact strength of PHBV/ENR blends. Data are presented as mean \pm SD. Groups designated with different letters are significantly different using One-Way ANOVA with Duncan's multiple range post hoc (at $p < 0.05$, $n = 3$).

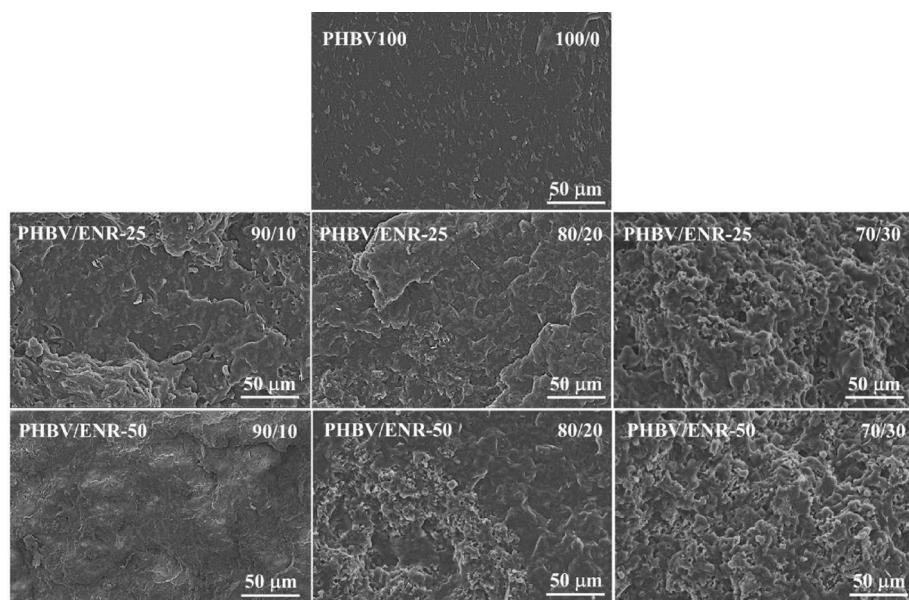


Figure 8. SEM micrographs of fractured surfaces of the neat PHBV, PHBV/ENR-25 blends, and PHBV/ENR-50 blends with the blending ratio of 90/10, 80/20, and 70/30.

ENR phases^{15,27}. The 70/30 PHBV/ENR-50 blend with 5 wt% PB-g-MA exhibited the most remarkable impact strength improvement. Different epoxide groups in natural rubber do not impact on toughness modification in various compositions. However, at 70/30 PHBV/ENR blends, the epoxide content seemed to impact the blends due to the good dispersion of rubber in the PHBV phase. In contrast, in other compositions, 10 wt% and 20 wt% ENR, the epoxide content had no significant effect on the toughness. The obtained results could be caused by the higher epoxide ring content that could promote PHBV chain scissions. To conclude, the PHBV/ENR blends with PB-g-MA addition improved mechanical attributes such as notched impact strength and strain at break, which could represent the successful approach for toughening PHBV.

Morphology. The morphology of the neat PHBV and PHBV/ENR blends was anticipated from their mechanical characteristics. As shown in Fig. 8, the fracture surface of the neat PHBV was quietly smooth, characteristic of brittle materials⁵², and lacked bonding due to the high crystallinity properties^{22,53}. The PHBV/ENR blends showed rough fracture surfaces with the presence of ductility materials^{54,55}. At small ENR contents (10–20 wt%), the fractured surfaces showed good dispersion and adhesion of ENR; although it is not possible to distinguish the PHBV phase and ENR phase, the obscure phase boundary could be confirmed, and no pulling out

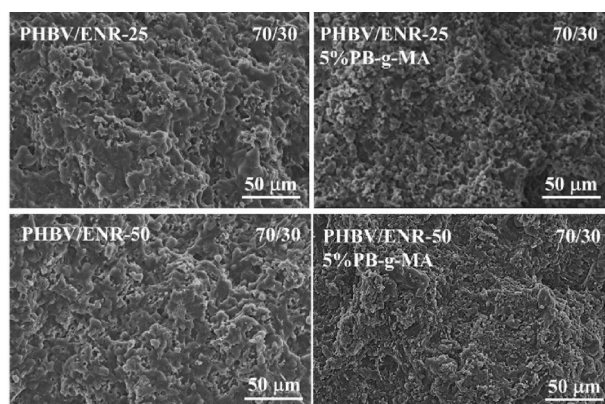


Figure 9. SEM micrographs of fractured surfaces of PHBV/ENR-25 and PHBV/ENR-50 blends with and without PB-g-MA.

of ENR phase for the blends containing 10–20 wt% of ENR. At larger ENR loading (30 wt%), the packed and folded morphology was observed with the ENR phase dispersed across the PHBV matrix. Also, the addition of 5 wt% PB-g-MA led to a smaller size of ENR dispersed in the PHBV matrix, as shown in Fig. 9. The 70/30 PHBV/ENR blends with and without 5 wt% PB-g-MA exhibited ductile fracture, supporting an extensive PHBV/ENR interacting network⁵⁶.

Biodegradable properties (soil burial test). Figure 10 presents the surface morphology of the neat PHBV (100 PHBV) and 70/30 PHBV/ENR blends with and without 5wt% PB-g-MA before being buried (0 months) and after buried (1, 2, and 3 months) in the compost soil⁵⁷. The neat PHBV exhibited a relatively smooth and clear surface before burial. However, after being buried for 1, 2, and 3 months in the compost soil, the samples showed different levels of degradation from the enzymatic action by living microorganisms in the compost soil.

As a result, a porous surface was developed and broken into small fragments related to the weight loss of the neat PHBV. After three months of being buried in the soil, the mass loss of PHBV was approximately 37%. Interestingly, the biodegradability of the blends was more pronounced, showing a mass reduction of approximately 40% and 45% for ENR-25 and ENR-50, respectively. This could be caused by the poor compatibility level of the blends²² and fragmented into smaller phases compared to the neat PHBV and the blends with 5wt% PB-g-MA due to the presence of PB-g-MA improved the compatibility between PHBV and ENR phases.

Conclusions

Epoxidized natural rubbers (ENRs) were effectively used to improve mechanical performance, particularly the toughness of PHBV. By melt blending process, the varying epoxide concentration of ENR (ENR-25 and ENR-50) has no significant influence on improving the impact property of the blends, while adding 5wt% polybutadiene grafted maleic anhydride (PB-g-MA) as a compatibilizer significantly affected. In this study, the favorable blending ratio delivering the highest toughness was 70/30 PHBV/ENR. The toughness of the blends with 5wt% PB-g-MA incorporation was approximately 200% greater than that of the neat PHBV. Furthermore, the biodegradability of PHBV/ENR blends was more substantial than that of neat PHBV, showing a mass reduction of approximately 40% and 45% for the blends ENR-25 and ENR-50, respectively. However, the mass loss of PHBV was approximately 37% after 3 months of soil burial. Consequently, the developed PHBV/ENR blends showed good properties for potential use as biodegradable packaging. Thus, using ENRs, derived from renewable resources for toughening PHBV could pave the way for broadening and diversifying ENRs and PHBV for eco-friendly and sustainable purposes.

Materials and methods

Materials. Poly(3-hydroxybutyrate-co-3-hydroxyvalerate) (PHBV, ENMAT Y1000P) was purchased from Ningbo Tianan Biologic Materials Co., Ltd., China. Epoxidized natural rubber with 25 and 50% epoxidation contents (ENR-25 and ENR-50) was purchased from Muang Mai Guthrie Pub Co., Ltd., Thailand. Polybutadiene grafted with maleic anhydride (PB-g-MA, Ricobond® 1756) was manufactured by Cray Valley LLC, USA. The PB-g-MA has a low molecular weight (2500) with the grafting of 3 MA groups per chain. The epoxidation natural rubber was used as received. However, PHBV pellets were dried at 60 °C for 24 h before usage, and PB-g-MA was stored in a desiccator to prevent moisture.

Preparation of PHBV/ENR blends. PHBV/ENR blends were prepared via the melt blending method using an internal mixer. The dried PHBV was first added in an internal mixer at a temperature of 175 °C with 50 rpm of rotating speed for 5 min to soften PHBV. Then, ENR and PB-g-MA were added, and the mixing was continued for another 5 min under the same conditions. The weight ratios of the PHBV to ENRs (ENR-25

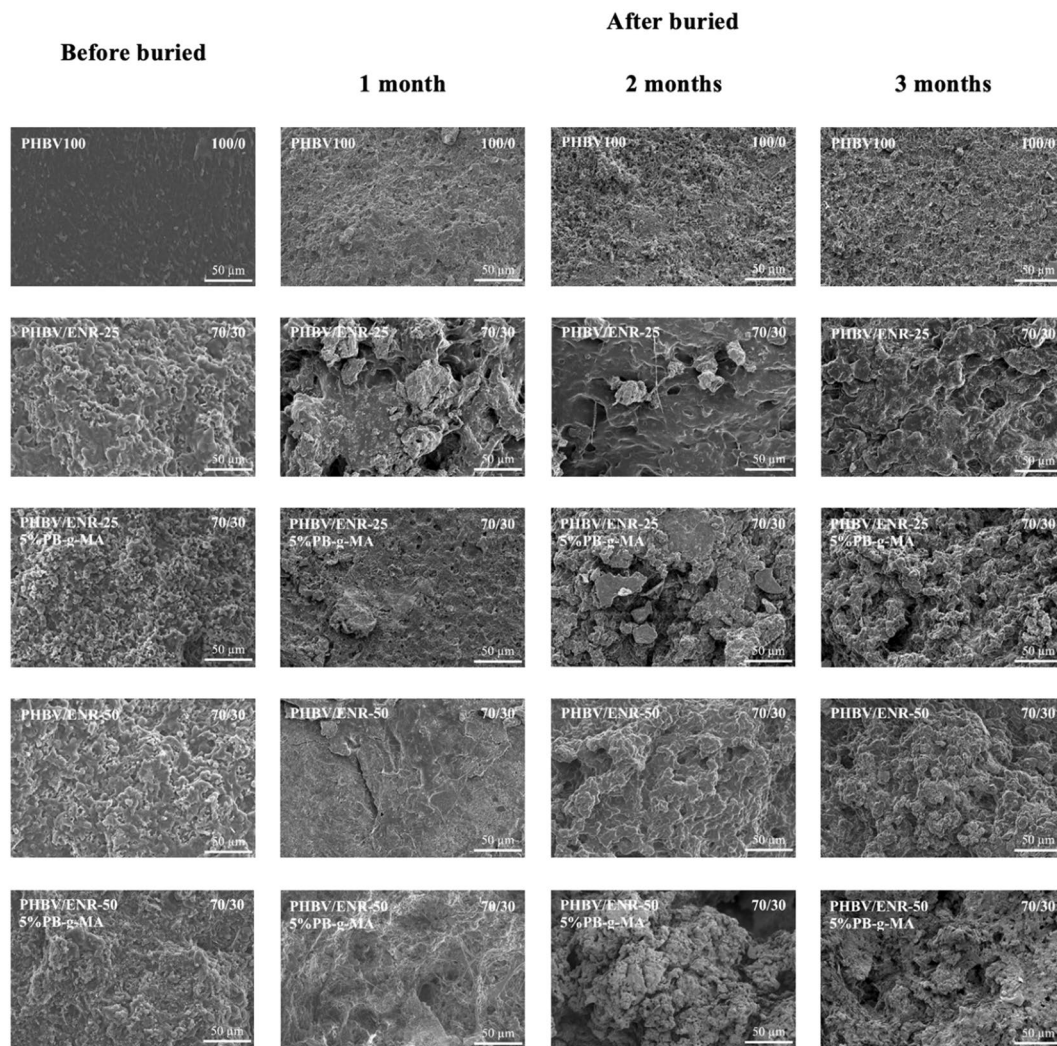


Figure 10. Representative SEM images of the neat PHBV, 70/30 PHBV/ENR-25 blends, and 70/30 PHBV/ENR-50 blends, with and without 5wt% PB-g-MA.

and ENR-50) were presented as follows: 100/0, 90/10, 80/20, and 70/30, with 5 and 10 wt% of PB-g-MA. The obtained PHBV/ENR blends were milled. Then, the standard test samples were formed using a compression molding machine operated at 180 °C.

Thermogravimetric analysis (TGA). The thermal stability of the PHBV pellet (unprocessed), ENR-25, ENR-50, and the PHBV/ENR blends with and without PB-g-MA were examined using STA 2500 (Netzsch, Germany). The samples were heated from room temperature to 600 °C at a heating rate of 10 °C min⁻¹ under N₂ atmosphere, and their thermal degradation temperatures (T_d) were determined.

Differential scanning calorimetry analysis (DSC). The thermal transitions of PHBV/ENR blends were investigated using 3500 Sirius (Netzsch, Germany). The samples were first heated from room temperature to 200 °C at a rate of 10 °C min⁻¹ under N₂ atmosphere and subsequently cooled to -70 °C at a cooling rate of 10 °C min⁻¹, then reheated from -70 to 200 °C with the same conditions and cool down into room temperature. The glass transition temperature (T_g), crystallization temperature (T_c), melting temperature (T_m), enthalpy of fusion (ΔH_m), and degree of crystallinity (X_c) were reported.

X-ray diffraction (XRD). XRD analysis of the neat PHBV and PHBV/ENR blends with and without PB-g-MA was performed using an X-ray diffractometer (D8 advance Bruker, USA). The XRD patterns were recorded in the range of 5–80°. The Scherrer's equation is used to calculate and determine the crystal size by $D = K\lambda / \beta \cos(\theta)^{-1}$, where D is the crystal size, K is the Scherrer's constant (0.9), λ is the wavelength of X-ray, β is full width half maximum; FWHM, θ is the scattering angle⁵⁸.

Mechanical characterization. Tensile testing was conducted according to ASTM D638 using standard dumbbell-shaped samples (type 4) with the dimensions of $6 \times 115 \times 3 \text{ mm}^3$ and a grip distance of 115 mm. The tensile testing was performed under the load cell capacity of 5 kN and a crosshead speed of 50 mm min^{-1} . Furthermore, the flexural testing was conducted according to ASTM D790 standard. The rectangle-shaped samples with the dimensions of $12.7 \times 127 \times 3 \text{ mm}^3$ were tested under the load cell capacity of 5 kN and a crosshead speed of 2 mm min^{-1} . The tensile and flexural tests were conducted using the universal testing machine Tinius Olsen H50KS (Calserve, Thailand). Moreover, the notched Izod impact testing was done according to ASTM D256 standard using the notched impact samples dimensions of $12.7 \times 63 \times 3 \text{ mm}^3$ with a 22.5° notched. All samples were notched using a notching machine (Taiwan Shang Yang, Taiwan), and the impact test was performed using an impact tester (Gotech, Taiwan). The standard test specimens for tensile testing, flexural testing, and impact testing were prepared via the compression molding process. The reported average and standard deviation (SD) values were calculated from at least five samples.

Statistical analysis. Statistical significance for the mechanical properties was determined using SPSS software (version 22.0; SPSS, Inc., Chicago, IL) using a one-way ANOVA with Duncan's multiple range post-hoc test. All data were obtained from triplicate measurements and presented as the mean \pm SD; P values < 0.05 were considered to be statistically significant.

Scanning electron microscopy (SEM). Blend morphology was examined via the fractured samples obtained from the impact testing using a scanning electron microscope (JSM – 6480LV, Jeol, Japan). Before being characterized, all samples were coated with gold using an SPI module sputter coater (Structure Probe, Inc., USA). Then, the SEM images were obtained with a voltage of 15 kV. Furthermore, the blend morphology evolution after biodegradation was also investigated. The samples obtained from the soil burial test were coated with gold, and the SEM images of the samples' surfaces were obtained with a voltage of 15 kV.

Biodegradability. For the biodegradability test, the 70/30 PHBV/ENR-50 blends with and without 5wt% of PB-g-MA and neat PHBV were selected as the most promising toughened blend composition and reference sample, respectively. According to the soil burial testing procedure, the samples were buried below the ground for 20 cm for 3 months^{59,60}. The burial test was performed in Bangkok, Thailand. At the desired time of 1, 2, and 3 months, the soil humidity is maintained at approximately 40%. After being buried at the desired time, the samples were subsequently taken off the soil, washed in distilled water, and dried in an oven at 60°C for 24 h. Then the samples were kept in a desiccator to prevent moisture.

Data availability

The datasets used and/or analyzed during the current study are available from the corresponding author on reasonable request.

Received: 7 June 2022; Accepted: 28 December 2022

Published online: 31 December 2022

References

- Mohammadpour Velni, S., Baniyasi, H. & Vaziri, A. Fabrication and characterization of antimicrobial starch-based nanocomposite films and modeling the process parameters via the RSM. *J. Polym. Compos.* **39**, E584–E591. <https://doi.org/10.1002/pc.24733> (2018).
- Githiru, M., Lens, L., Adriaensens, F., Mwang'ombe, J. & Matthysen, E. Using science to guide conservation: From landscape modeling to increased connectivity in the Taita Hills SE, Kenya. *J. Nat. Conserv.* **19**, 263–268. <https://doi.org/10.1016/j.jnc.2011.03.002> (2011).
- Siracusa, V. & Blanco, I. Bio-polyethylene (Bio-PE), bio-polypropylene (Bio-PP) and bio-poly (ethylene terephthalate)(Bio-PET): Recent developments in bio-based polymers analogous to petroleum-derived ones for packaging and engineering applications. *J. Polym.* **12**, 1641. <https://doi.org/10.3390/polym12081641> (2020).
- Ayyubi, S. N. & Purbasari, A. The effect of composition on mechanical properties of biodegradable plastic based on chitosan/cassava starch/PVA/crude glycerol: Optimization of the composition using box behnken design. *Mater. Today: Proc.* <https://doi.org/10.1016/j.matpr.2022.01.294> (2022).
- Holmes, P. Applications of PHB-a microbially produced biodegradable thermoplastic. *J. Phys. Technol.* **16**, 32. <https://doi.org/10.1088/0305-4624/16/1/305> (1985).
- Bhatt, R., Shah, D., Patel, K. & Trivedi, U. PHA-rubber blends: Synthesis, characterization and biodegradation. *J. Bioresour. Technol.* **99**, 4615–4620. <https://doi.org/10.1016/j.biortech.2007.06.054> (2008).
- Chen, G.-Q., Hajnal, I., Wu, H., Lv, L. & Ye, J. Engineering biosynthesis mechanisms for diversifying polyhydroxyalkanoates. *Trends. Biotechnol.* **33**, 565–574. <https://doi.org/10.1016/j.tibtech.2015.07.007> (2015).
- Lenz, R. W. & Marchessault, R. H. Bacterial polyesters: Biosynthesis, biodegradable plastics and biotechnology. *J. Biomacromolecules* **6**, 1–8. <https://doi.org/10.1021/bm049700c> (2005).
- Tomano, N., Boondamnoen, O., Aumnate, C., Potiyaraj, P. In *J. Phys. Conf. Ser.* 012026 (IOP Publishing).
- Anderson, A. J. & Dawes, E. Occurrence, metabolism, metabolic role, and industrial uses of bacterial polyhydroxyalkanoates. *J. Microbiol. Rev.* **54**, 450–472. <https://doi.org/10.1128/mr.54.4.450-472.1990> (1990).
- Yeo, J. C. C., Muiruri, J. K., Thitsartarn, W., Li, Z. & He, C. Recent advances in the development of biodegradable PHB-based toughening materials: Approaches, advantages and applications. *J. Mater. Sci. Eng. C.* **92**, 1092–1116. <https://doi.org/10.1016/j.msec.2017.11.006> (2018).
- Bugnicourt, E., Cinelli, P., Lazzeri, A. & Alvarez, V. A. Polyhydroxyalkanoate (PHA): Review of synthesis, characteristics, processing and potential applications in packaging. *Express Polym. Lett.* <https://doi.org/10.3144/expresspolymlett.2014.82> (2014).
- Hedrick, M. M., Wu, F., Mohanty, A. K. & Misra, M. Morphology and performance relationship studies on biodegradable ternary blends of poly (3-hydroxybutyrate-co-3-hydroxyvalerate), polylactic acid, and polypropylene carbonate. *RSC Adv.* **10**, 44624–44632. <https://doi.org/10.1039/D0RA07485C> (2020).

14. Kennouche, S. *et al.* Morphological characterization and thermal properties of compatibilized poly (3-hydroxybutyrate-co-3-hydroxyvalerate)(PHBV)/poly (butylene succinate)(PBS)/halloysite ternary nanocomposites. *J. Eur. Polym. Sci.* **75**, 142–162. <https://doi.org/10.1016/j.eurpolymj.2015.12.009> (2016).
15. Lee, H., Ismail, J., Kammer, H. & Bakar, M. A. Melt reaction in blends of poly (3-hydroxybutyrate)(PHB) and epoxidized natural rubber (ENR-50). *J. Appl. Polym. Sci.* **95**, 113–129. <https://doi.org/10.1002/app.20808> (2005).
16. Ma, P., Hristova-Bogaerds, D. G., Lemstra, P. J., Zhang, Y. & Wang, S. Toughening of PHBV/PBS and PHB/PBS blends via in situ compatibilization using dicumyl peroxide as a free-radical grafting initiator. *J. Macromol. Mater. Eng.* **297**, 402–410. <https://doi.org/10.1002/mame.201100224> (2012).
17. Javadi, A. *et al.* Processing and characterization of microcellular PHBV/PBAT blends. *J. Polym. Eng. Sci.* **50**, 1440. <https://doi.org/10.1002/pen.21661> (2010).
18. Jaratrotkamjorn, R., Khaokong, C. & Tanrattanakul, V. Toughness enhancement of poly (lactic acid) by melt blending with natural rubber. *J. Appl. Polym. Sci.* **124**, 5027–5036. <https://doi.org/10.1002/app.35617> (2012).
19. Baker, C., Gelling, I. & Newell, R. Epoxidized natural rubber. *J. Rubber Chem. Technol.* **58**, 67–85. <https://doi.org/10.5254/1.3536059> (1985).
20. Tanjung, F. A., Hassan, A. & Hasan, M. Use of epoxidized natural rubber as a toughening agent in plastics. *J. Appl. Polym. Sci.* <https://doi.org/10.1002/app.42270> (2015).
21. Chutamas, M., Sunthornvarabhas, J., Hyun, J. K., Klanarong, S. In *Advanced Materials Research*. 179–182 (Trans Tech Publ).
22. Parulekar, Y. & Mohanty, A. K. Biodegradable toughened polymers from renewable resources: Blends of polyhydroxybutyrate with epoxidized natural rubber and maleated polybutadiene. *J. Green Chem.* **8**, 206–213. <https://doi.org/10.1039/B508213G> (2006).
23. Ramachandran, A. A., Mathew, L. P. & Thomas, S. Effect of MA-g-PP compatibilizer on morphology and electrical properties of MWCNT based blend nanocomposites: New strategy to enhance the dispersion of MWCNTs in immiscible poly (trimethylene terephthalate)/polypropylene blends. *J. Eur. Polym.* **118**, 595–605. <https://doi.org/10.1016/j.eurpolymj.2019.06.027> (2019).
24. Parulekar, Y., Mohanty, A. K. & Imam, S. H. Biodegradable nanocomposites from toughened polyhydroxybutyrate and titanate-modified montmorillonite clay. *J. Nanosci. Nanotechnol.* **7**, 3580–3589. <https://doi.org/10.1166/jnn.2007.852> (2007).
25. Parulekar, Y. S. & Mohanty, A. K. In *Society of Plastics Engineers Automotive Composites Conference*.
26. Ma, P. *et al.* Styrene-assisted melt free-radical grafting of maleic anhydride onto poly (β -hydroxybutyrate). *J. Polym. Degrad. Stab.* **100**, 93–100. <https://doi.org/10.1016/j.polyimdegradstab.2013.12.005> (2014).
27. Algaily, B., Kaewsakul, W., Sarkawi, S. S. & Kalkornsurasranee, E. Enabling reprocessability of ENR-based vulcanisates by thermochemically exchangeable ester crosslinks. *J. Plast. Rubber Compos.* **50**, 315–328. <https://doi.org/10.1080/14658011.2021.1896093> (2021).
28. Nakason, C., Wannavilai, P. & Kaesaman, A. Effect of vulcanization system on properties of thermoplastic vulcanisates based on epoxidized natural rubber/polypropylene blends. *J. Polym. Test.* **25**, 34–41. <https://doi.org/10.1016/j.polymertesting.2005.09.007> (2006).
29. Harun, F. & Chan, C. H. In *Flexible and Stretchable Electronic Composites* 37–59 (Springer, 2016).
30. Arun, A., Arthi, R., Shanmugabalaji, V. & Eyini, M. Microbial production of poly- β -hydroxybutyrate by marine microbes isolated from various marine environments. *J. Bioresour. Technol.* **100**, 2320–2323. <https://doi.org/10.1016/j.biortech.2008.08.037> (2009).
31. Zhao, X., Cornish, K. & Vodovotz, Y. Synergistic mechanisms underlie the peroxide and coagent improvement of natural-rubber-toughened poly (3-hydroxybutyrate-co-3-hydroxyvalerate) mechanical performance. *J. Polym.* **11**, 565. <https://doi.org/10.3390/polym11030565> (2019).
32. He, J. D., Cheung, M. K., Yu, P. H. & Chen, G. Q. Thermal analyses of poly (3-hydroxybutyrate), poly (3-hydroxybutyrate-co-3-hydroxyvalerate), and poly (3-hydroxybutyrate-co-3-hydroxyhexanoate). *J. Appl. Polym. Sci.* **82**, 90–98. <https://doi.org/10.1002/app.1827> (2001).
33. Wang, S. *et al.* Characteristics and biodegradation properties of poly (3-hydroxybutyrate-co-3-hydroxyvalerate)/organophilic montmorillonite (PHBV/OMMT) nanocomposite. *J. Polym. Degrad. Stab.* **87**, 69–76. <https://doi.org/10.1016/j.polyimdegradstab.2004.07.008> (2005).
34. He, C., Wang, Y., Luo, Y., Kong, L. & Peng, Z. Thermal degradation kinetics and mechanism of epoxidized natural rubber. *J. Polym. Eng.* **33**, 331–335. <https://doi.org/10.1515/polyeng-2013-0040> (2013).
35. Zhang, K., Misra, M. & Mohanty, A. K. Toughened sustainable green composites from poly (3-hydroxybutyrate-co-3-hydroxyvalerate) based ternary blends and miscanthus biofiber. *ACS Sustain. Chem. Eng.* **2**, 2345–2354. <https://doi.org/10.1021/sc500353v> (2014).
36. Harrison, I. R. & Runt, J. Incompatible blends: Thermal effects in a model system. *J. Polym. Sci. Polym. Phys.* **18**, 2257–2261. <https://doi.org/10.1002/pol.1980.180181109> (1980).
37. Lisowski, M. S. *et al.* Crystallization behavior of poly (ethylene oxide) and its blends using time-resolved wide- and small-angle X-ray scattering. *J. Macromolecules* **33**, 4842–4849. <https://doi.org/10.1021/ma000207c> (2000).
38. Babu, R. R., Singha, N. K. & Naskar, K. Dynamically vulcanized blends of polypropylene and ethylene octene copolymer: Influence of various coagents on mechanical and morphological characteristics. *J. Appl. Polym. Sci.* **113**, 3207–3221. <https://doi.org/10.1002/app.32023> (2009).
39. Dawidziuk, K. A. *Peroxide-initiated modification of polylactic acid (PLA) and poly (3-hydroxyalkanoates)(PHAs) in the presence of allylic and acrylic coagents* (Queen's University, Canada, 2018).
40. Zhao, X., Venoor, V., Koelling, K., Cornish, K. & Vodovotz, Y. Bio-based blends from poly (3-hydroxybutyrate-co-3-hydroxyvalerate) and natural rubber for packaging applications. *J. Appl. Polym. Sci.* **136**, 47334 (2019).
41. Naphade, R. & Jog, J. Electrospinning of PHBV/ZnO membranes: Structure and properties. *J. Fibers Polym.* **13**, 692–697. <https://doi.org/10.1007/s12221-012-0692-9> (2012).
42. Xu, H. & Van Deventer, J. S. Microstructural characterisation of geopolymers synthesised from kaolinite/stilbite mixtures using XRD, MAS-NMR, SEM/EDX, TEM/EDX, and HREM. *J. Cem. Concr. Res.* **32**, 1705–1716. [https://doi.org/10.1016/S0008-8846\(02\)00859-1](https://doi.org/10.1016/S0008-8846(02)00859-1) (2002).
43. Thayer, T. A., Bagby, M. D., Moore, R. N. & DeAngelis, R. J. X-ray diffraction of nitinol orthodontic arch wires. *Am. J. Orthod. Dentofac. Orthop.* **107**, 604–612. [https://doi.org/10.1016/S0889-5406\(95\)70103-6](https://doi.org/10.1016/S0889-5406(95)70103-6) (1995).
44. Bartczak, Z. & Galeski, A. Mechanical properties of polymer blends. *Polym. Blends Handb.* https://doi.org/10.1007/978-94-007-6064-6_13 (2014).
45. Thomason, J. The influence of fibre length, diameter and concentration on the impact performance of long glass-fibre reinforced polyamide 6, 6. *J. Compos. A Appl. Sci. Manuf.* **40**, 114–124. <https://doi.org/10.1016/j.compositesa.2008.10.013> (2009).
46. Kuntanoo, K., Promkotra, S. & Kaewkannetra, P. Biodegradation of polyhydroxybutyrate-co-hydroxyvalerate (PHBV) blended with natural rubber in soil environment. *Int. Sci. Index* **7**, 12. <https://doi.org/10.5281/zenodo.1087696> (2013).
47. Modi, S. J., Cornish, K., Koelling, K. & Vodovotz, Y. Fabrication and improved performance of poly (3-hydroxybutyrate-co-3-hydroxyvalerate) for packaging by addition of high molecular weight natural rubber. *J. Appl. Polym. Sci.* <https://doi.org/10.1002/app.43937> (2016).
48. Kaynak, C., Arikan, A. & Tincer, T. Flexibility improvement of short glass fiber reinforced epoxy by using a liquid elastomer. *J. Polym.* **44**, 2433–2439. [https://doi.org/10.1016/S0032-3861\(03\)00100-9](https://doi.org/10.1016/S0032-3861(03)00100-9) (2003).
49. Plotino, G., Grande, N. M., Bedini, R., Pameijer, C. H. & Somma, F. Flexural properties of endodontic posts and human root dentin. *J. Dent. Mater.* **23**, 1129–1135. <https://doi.org/10.1016/j.dental.2006.06.047> (2007).

50. Liang, J. & Li, R. Rubber toughening in polypropylene: A review. *J. Appl. Polym. Sci.* **77**, 409–417. [https://doi.org/10.1002/\(SICI\)1097-4628\(20000711\)77:2%3c409::AID-APP18%3e3.0.CO;2-N](https://doi.org/10.1002/(SICI)1097-4628(20000711)77:2%3c409::AID-APP18%3e3.0.CO;2-N) (2000).
51. Rodgers, B. *Rubber compounding: Chemistry and applications* (CRC Press, 2015).
52. Liu, G.-C., He, Y.-S., Zeng, J.-B., Xu, Y. & Wang, Y.-Z. In situ formed crosslinked polyurethane toughened polylactide. *J. Polym. Chem.* **5**, 2530–2539. <https://doi.org/10.1039/C3PY01649H> (2014).
53. Takayanagi, M., Uemura, S., Minami, S. In *J. Polym. Sci., Part C: Polym. Symp.* 113–122 (Wiley Online Library).
54. D'orazio, L. *et al.* Effect of the addition of ethylene-propylene random copolymers on the properties of high-density polyethylene/isotactic polypropylene blends: Part 1—morphology and impact behavior of molded samples. *J. Polym. Eng. Sci.* **22**, 536–544. <https://doi.org/10.1002/pen.760220904> (1982).
55. Wang, Y., Chen, K., Xu, C. & Chen, Y. Supertoughened biobased poly (lactic acid)–epoxidized natural rubber thermoplastic vulcanizates: Fabrication, co-continuous phase structure, interfacial in situ compatibilization, and toughening mechanism. *J. Phys. Chem. B* **119**, 12138–12146. <https://doi.org/10.1021/acs.jpcc.5b06244> (2015).
56. Zhang, K., Nagarajan, V., Misra, M. & Mohanty, A. K. Supertoughened renewable PLA reactive multiphase blends system: Phase morphology and performance. *ACS Appl. Mater. Interfaces* **6**, 12436–12448. <https://doi.org/10.1021/am502337u> (2014).
57. Chee, W. K., Ibrahim, N. A., Zainuddin, N., Abd Rahman, M. F. & Chieng, B. W. Impact toughness and ductility enhancement of biodegradable poly (lactic acid)/poly (ϵ -caprolactone) blends via addition of glycidyl methacrylate. *J. Adv. Mater. Sci. Eng.* <https://doi.org/10.1155/2013/976373> (2013).
58. Uvarov, V. & Popov, I. Metrological characterization of X-ray diffraction methods at different acquisition geometries for determination of crystallite size in nano-scale materials. *J. Mater. Charact.* **85**, 111–123. <https://doi.org/10.1016/j.matchar.2013.09.002> (2013).
59. Chaiwutthinan, P., Chauyuljit, S., Thipkham, N., Kowalski, C. P. & Boonmahitthisud, A. Poly (lactic acid)/ethylene vinyl acetate copolymer blend composites with wood flour and wollastonite: Physical properties, morphology, and biodegradability. *J. Vinyl Addit. Technol.* **25**, 313–327. <https://doi.org/10.1002/vnl.21697> (2019).
60. Chauyuljit, S., Kongthan, J., Chaiwutthinan, P. & Boonmahitthisud, A. Poly (vinyl chloride)/poly (butylene succinate)/wood flour composites: Physical properties and biodegradability. *J. Polym. Compos.* **39**, 1543–1552. <https://doi.org/10.1002/pc.24098> (2018).

Acknowledgements

We acknowledge the financial support from the National Science and Technology Development Agency of Thailand (#P-19-51362), the Southeast Asia – Europe Joint Funding Scheme for Research and Innovation (Project BIOPATE) and Chulalongkorn University: CU_GR_63_68_23_12. Napat Tomano would like to acknowledge the Second Century Fund (C2F), Chulalongkorn university for the support. We also thanks Department of Materials Science, Faculty of Science and Metallurgy and Materials Science Research Institute, Chulalongkorn University for providing the research facilities to make this research possible.

Author contributions

N.T.: Methodology, Investigation, Writing- Original draft preparation; O.B.: Conceptualization, Methodology, Data curation, Writing- Original draft preparation, Writing-Reviewing and Editing; C.A.: Conceptualization, Methodology, Data curation, Writing- Original draft preparation, Writing-Reviewing and Editing; P.P.: Resources, Supervision, Writing-Reviewing and Editing.

Competing interests

The authors declare no competing interests.

Additional information

Correspondence and requests for materials should be addressed to O.B. or C.A.

Reprints and permissions information is available at www.nature.com/reprints.

Publisher's note Springer Nature remains neutral with regard to jurisdictional claims in published maps and institutional affiliations.



Open Access This article is licensed under a Creative Commons Attribution 4.0 International License, which permits use, sharing, adaptation, distribution and reproduction in any medium or format, as long as you give appropriate credit to the original author(s) and the source, provide a link to the Creative Commons licence, and indicate if changes were made. The images or other third party material in this article are included in the article's Creative Commons licence, unless indicated otherwise in a credit line to the material. If material is not included in the article's Creative Commons licence and your intended use is not permitted by statutory regulation or exceeds the permitted use, you will need to obtain permission directly from the copyright holder. To view a copy of this licence, visit <http://creativecommons.org/licenses/by/4.0/>.

© The Author(s) 2022